Journal of Chemical Health Risks

Journal of Chemical Health Risks (2016) 6(3), 203-212

ORIGINAL ARTICLE

Synthesis of Hydroxyapatite/Ag/TiO_2 Nanotubes and Evaluation of Their Anticancer Activity on Breast Cancer Cell Line MCF-7

Sara Rahimnejad[*1], Maryam Bikhof Torbati[*2]

[1]Department of Chemistry, College of Basic science, Yadegar-e-Imam Khomeini (RAH) Shahre Rey Branch, Islamic Azad University, Tehran, Iran

[2]Department of Biology, College of Basic Science, Yadegar-e-Imam Khomeini(RAH) Shahre Rey Branch, Islamic Azad University, Tehran, Iran

(Received: 30 January 2016 Accepted: 6 April 2016)

KEYWORDS

Hydroxyapatite;
Nanotube;
TiO_2;
Anticancer;
Breast cancer;
MCF-7

ABSTRACT: In this research, TiO_2 nanotubes were synthesized by anodized oxidation method and were covered with a hydroxyapatite-silver nanoparticles using photodeposition and dip coating for loading silver nanoparticles and coated hydroxyapatite (HA). The morphological texture of TiO_2 nanotube and Ag-HA nanoparticles on TiO_2 nanotubes surface were studied by field emission scanning electron microscopy (FESEM), energy dispersive X-ray spectroscopy (EDAX analysis) and X-ray diffraction (XRD). The MCF-7 cell lines were treated with concentrations 1, 10 and 100 µg/ml of TiO_2 nanotubes and HA/Ag/TiO_2 nanotube for 24 and 48h. Finally, the cell viability and IC50% were evaluated using MTT assay. The results show that the HA/Ag/TiO_2 has more positive effect on enhancing the cell death compare to TiO_2 nanotubes and also exerts a time and concentration-dependent inhibition effect on viability of MCF-7 cells.

INTRODUCTION

In recent years, there has been steady advancement in the biomedical field [1]. In recent times much attention has been focused on Titania and Ti alloys. The nanotubular Titania is of a promising and important prospect in solar cells [2, 3], environmental purification [4], photolysis water [5], gas sensor [6, 7] and bio-application [8, 9] due to its unique highly ordered array structure, good mechanical and chemical stability, excellent corrosion resistance, high specific surface area and biocompatibility. However, in order to improve its biocompatibility, Titania surface should be modified. The particular morphology of nanoscale can affect

* Corresponding author:sara.rahimnejad@gmail.com; maryam.bikhof@gmail.com (S. Rahimnejad & M. Bikhof Torbati).

surface roughness and increase the strength of adhesion and spreading and proliferation of cells on the nano-structured titanium. High energy level also associated with increased levels of nano raw surface protein intake to the level of the cell interaction. Therefore, the distribution of surface charge and chemistry can play an important role in cell adhesion on the surface. One of the important advantages of Titanium dioxide nanotubes survey related to the adhesion, growth and differentiation of cells other than Titanium nanostructures that these features would ultimately increase cell death [9]. Adhesion, spreading, growth, and differentiation of mesenchymal stem cells are critically dependent on the tube diameter of vertically oriented TiO_2 nanotubes [10].

On the other hand, MCF-7 breast cancer cells treated with colloidal silver, significantly reduced the dehydrogenase activity, resulting in decreased $NADH/NAD^+$, which in turn induces cell death due to decreased mitochondrial membrane potential [11].

Effect of hydroxyapatite (HA) particles on the survival of gastric cancer cells of SGC-7901, nano-hydroxyapatite significantly decreased cell viability and induction of apoptosis in these cells so that the DNA fragment and morphological changes occur in cells [12].

In this paper we wish to disclose our initial results on the synthesis of composite TiO_2 nanotube covered with HA and silver, their uniform dispersed chemical surface as anticancer drug on MCF-7 cells line and finally their cytotoxicity studies. Anodization method in combination with photodeposition and dip coating method was employed as convenient method for the preparation $HA/Ag/TiO_2$ nanotube. Field Emission Scanning Electron Microscopy and X-Ray Diffraction were used to study the morphology and crystallinity of the $HA/Ag/TiO_2$. FT IR studies have confirm the loading of hydroxyapatite onto the TiO_2 nanotube. Finally cell viability was measured on MCF-7 cells using a MTT assay.

MATERIALS AND METHODS

Synthesis of titanium dioxide nanotube arrays

High-purity titanium foil (99.6%, 0.5 mm thick) was sonicated in acetone, isopropanol for 30 sec. The cleaned titanium foils were anodized at a constant potential of 60 V in an ethylene glycol solution containing 0.3 wt% NH_4F and 2vol%H_2O for 30 min in a two-electrode configuration with a Platinium cathode [13].

After anodic oxidation, the samples were rinsed with ethanol and water and dried in air. The resulting amorphous Titania nanotube arrays were annealed at 500 °C for 3 h with heating and cooling rates of 2 °C min^{-1} in air to crystallize the tube walls and improve their activity.

The structures of the anoized TiO_2 nanotube arrays were characterized by scanning electron microscopy (SEM, XL 30 Philips company). X-Ray diffraction studies were carried out with an X-ray diffractometer (Philips X'Pert) using Cu kα radiation. The FT IR spectra of the sample were recorded on a Bruker FTIR 27 Tensor spectrometer. The spectra were recorded from 400-4000 cm^{-1}.

Deposition of silver nanoparticles on titanium dioxide nanotube

In order to prepare Ag nanoparticles deposited on TiO_2, a silver nitrate ($AgNO_3$) aqueous solution with a concentration of 0.014 M was prepared. The TiO_2 nanotube film was dipped on this solution. These samples were dried at room temperature after dipping for 30 min and irradiated under UV light (at 254 nm) from a G15W/T8 Sylvania tube lamp for 2 h.

The silver metal was photoreduced and fixed onto the TiO_2 surface by a photodeposition operation. The samples were washed ultrasonically twice in deionized water to obtain the high purity samples for the next procedure which coated the hydroxyapatite [14].

Deposition of hydroxyapatite on Silver loaded Titanium dioxide

For coating hydroxyapatite particles on silver deposited titanium dioxide nanotube, the modified TiO_2 nanotube film was immersed on an aqueous solution of 0.1 M hydroxyapatite for 30 min. Then white solid appeared and the sample was dried on air [15].

Cell culture

MCF-7 cells (NCBI C135, National Cell Bank of Iran), were obtained from Pasteur Institute of Iran and cultured in standard culture medium, which consisted of Dulbecco's Modified Eagle Medium (DMEM) supdplemented with 2 mM Glutamine, antibiotics (100 U/l penicillin, 100 µg/ml streptomycin) and 10% fetal bovine serum (FBS) and incubated at 37 °C in a humidified 5% CO_2 atmosphere.

Stock solutions of the studied TiO_2 nanotube and $HA/Ag/TiO_2$ nanocomposit were prepared in dimethyl sulfoxide (DMSO, Sigma Aldrich) at a concentration of 1000 µg/mL, then sonicated for 4 h to achive a homogenous suspention of nanocomposite and sterilized by filtration through Millipore filter, 0.22 µm, before use, and diluted by cell culture medium to various working concentration. The DMSO solvent was used due to solubility problems.

MCF-7 cells were seeded (5000 cells per well) into 96 - wells flat-bottom microtiter plates and incubated for 4 h prior to the addition of filtered 3 different concentrations of the studied compounds. Final concentrations achieved in treated wells were 0.1, 1 and 100 µg/mL. Each concentration was tested in quadruplicate on each cell line. The final concentrations (<0.1%) of DMSO, were non-toxic to the cells. Only complete medium was added to the cells in the control wells. The incubation time was 24 and 48 h, during the period the control cells showed exponential growth.

MTT assay

The evaluation of the MCF-7 cells survival and proliferation was done using the tetrazolium-based colorimetric assay (MTT) [16] and modified later [17]. MTT (3 - [4, 5-dimethylthiazol – 2 - yl] - 2, 5 - diphenyltetrazolium bromide; SIGMA) is a yellow water-soluble tetrazolium dye reduced by live cells into a purple formazan product insoluble in aqueous sloution . Briefly, cells were incubated for 24 and 48 h and then, 20 µl of MTT solution (5 mg/mL) in phosphate buffer saline (1/10 of total volume in a well) was added to wells. The MCF-7 cells were incubated for 4 h in humified atmosphere (5% CO_2) in the dark. Afterward, the supernatants were removed and the purple crystals were solubilized in 100 µL of DMSO. The plate was shaken for 15 min by a shaker incubator in order to dissolve the formazan crystals. The absorbance was measured at wavelengths of 570, 630 nm in an ELISA plate (Stat Fax-2100, USA) reader. The results were reported the average of 3 replications and expressed as cytotoxicity and viability percenatge by the following equation:

$$\% \text{ Cytotoxicity} = \frac{\text{absorbence of toxicant}}{\text{absorbence of negative control}} \times 100$$

% Viability = 100 - % Cytotoxicity

RESULTS AND DISCUSSION

Figure 1 shows FESEM images of TiO_2 nanotube (TNT) fabricated in EG-based electrolyte at 60 V for 30 min after anodization. The TNT with open mouth-tube morphology was obtained after optimized ultrasonic agitation (Figure 1a). The image indicates that the TiO_2 NT have an inner pore diameter of approximately 100 nm, average wall diameter of 45 nm and well aligned NTs vertically oriented from the Ti foil substrate. The

presence of well-aligned TNTs would promote direct charge transport. Therefore, the well-oriented TNTs may present the role of make distribution of surface charge on TNTs morphologies and subsequently effect on cell adhesion on the surface. Figure 1b shows the bottom surface morphology of TNT after Peeling off from underlying Ti substrate. The image shows that TNTs are closed at bottom surface.

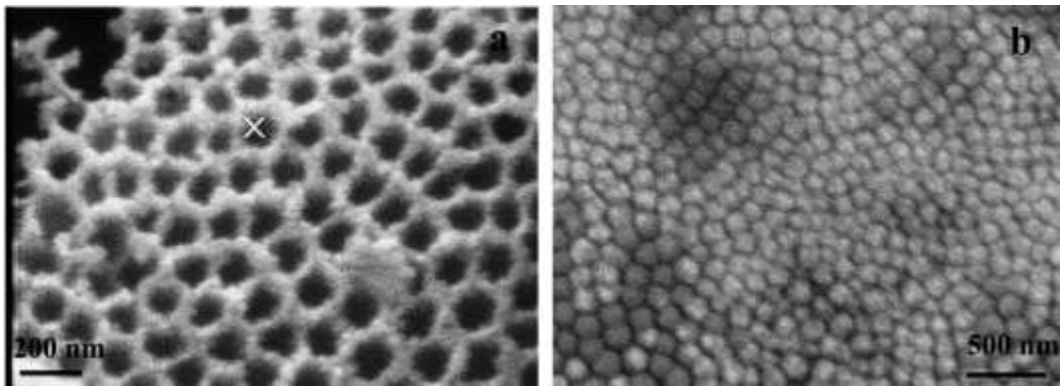

Figure 1. FESEM images of TiO_2 nanotubes fabricated in EG containing 0.3 wt% NH_4F and 2 Vol% H_2O via anodization: (a) top surface view, (b) bottom surface view of Ti-substrate after separation of TiO_2 nanotubes

The energy dispersive X-ray (EDX) spectrometry clearly shows the presence of Ti, Ag, Ca, and P elements on the surface of catalyst. Figure 2A indicates the presence of Ag nanoparticle on TiO_2 nanotubes. In Figure 2B, the presence of hydroxyapatite (the ratio Ca/P is 1.64) is clear [18, 19].

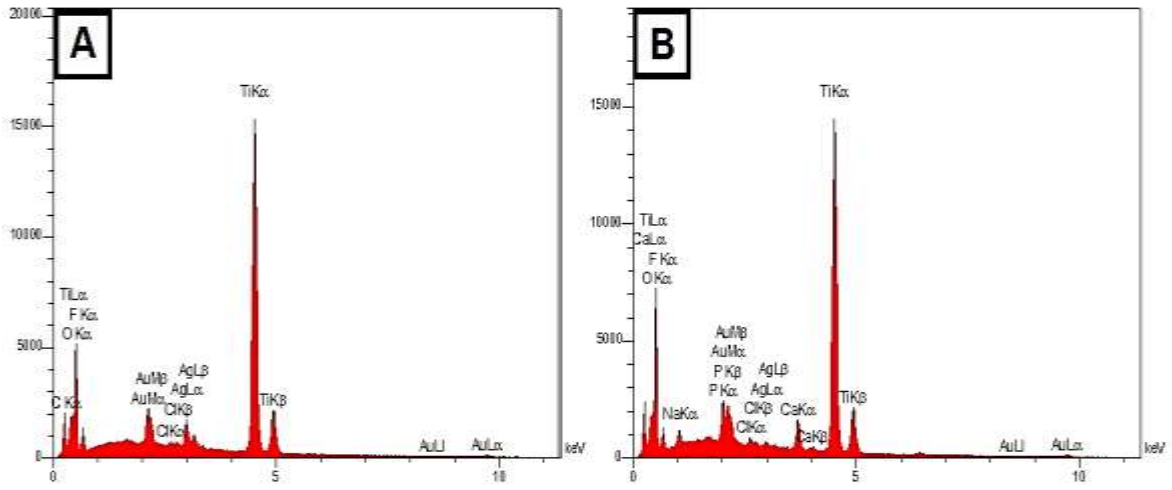

Figure 2. Energy dispersive X-ray spectroscopy (EDX) spectra of (a) Ag/TNT (b) HA/Ag/TNT

Figure 3a shows the X-ray diffraction patterns of TNT in the range of 5-70 °C. The appearance of sample diffraction peaks at 2θ= 25.4°, 38.3°, 48.1°, 54° and 62.7° are corresponding to the anatase phase. In Figure 3b, the three dominant peaks such as (211) (2θ = 31.8˚), (112) (2θ = 32.2˚), and (300) (2θ = 32.9˚) indicate the presence of hydroxyapatite particle with the structure of hexagonal crystal which are verified by comparing data obtained with the PDF (Powder Diffraction File) pattern 09-0432. For the composite HA/Ag/TiO_2, no crystalline phase of silver formation was observed. This may due to the uniform distribution of silver nanoparticles in the

titanium dioxide surface, or related to the peak of silver at 2θ=38.4° was overlapped by the diffraction peak of TiO_2 at 38.3° owing to the less content of silver [20].

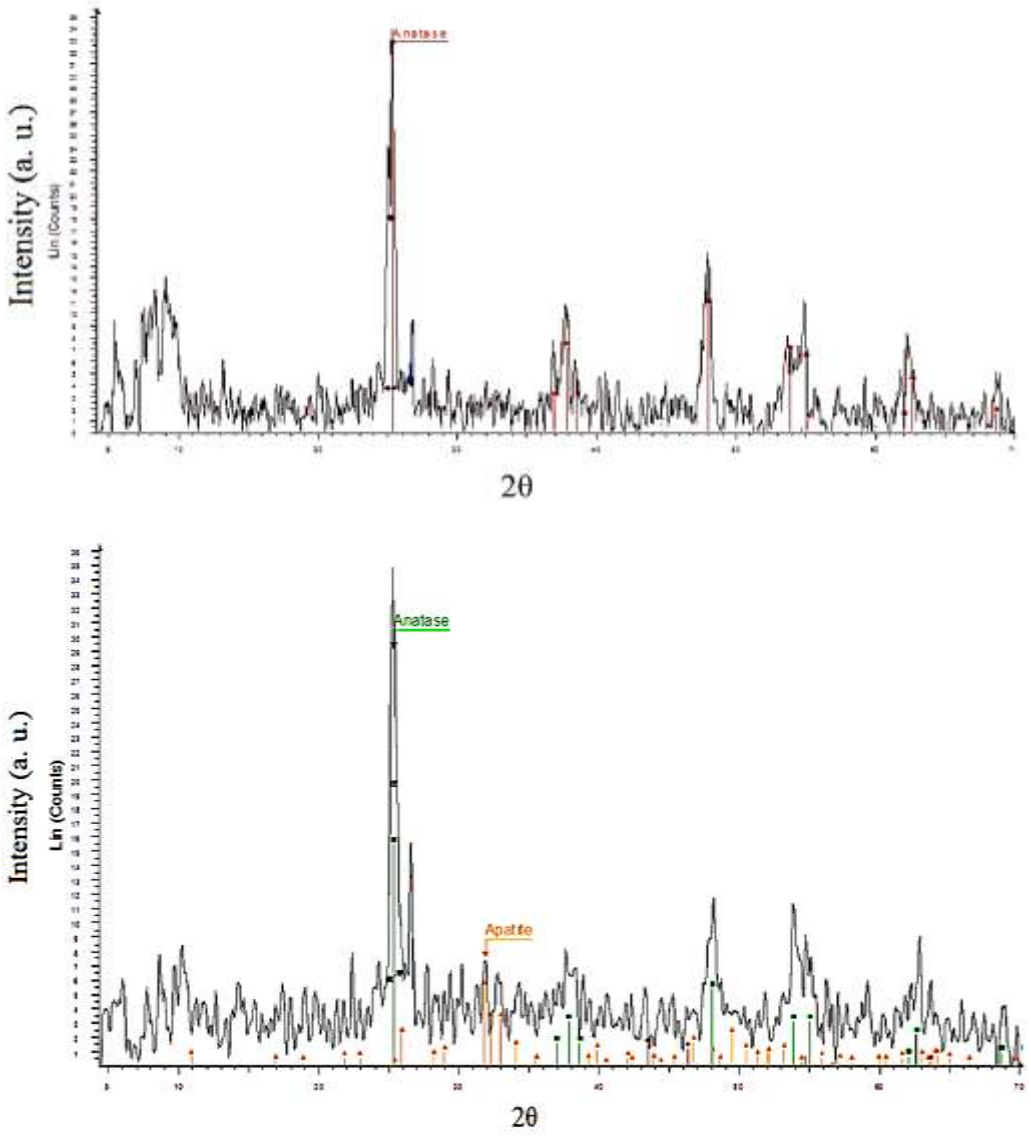

Figure 3. The X-ray diffraction (XRD) pattern of a) TiO2 nanotube (TNT), and b) HA/Ag/TiO2 thermal treated at 500 □C for 3 h

Interaction and binding of hydroxyapatite particles to TNT was confirmed by taking FTIR spectra (Figure 4). The FTIR spectrum of HA/Ag/TiO_2 NT showed characteristic peaks at 1042 cm^{-1} and 1096 cm^{-1} for P-O stretching and the orthophosphate (PO_4^{3-}) stretching mode was also observed at 602 cm^{-1} and 570 cm^{-1}. The phosphate bands are identified by peaks at ~962cm^{-1}. The other peaks related to TiO_2 are observed in the sample. The broad band centered at 500-600 cm^{-1} is likely due to the vibration of the Ti–O bonds in the TiO_2 lattice. The peaks at 1620-1630 cm^{-1} and the broad

peaks appearing at 3100–3600 cm^{-1} are assigned to vibrations of OH groups.

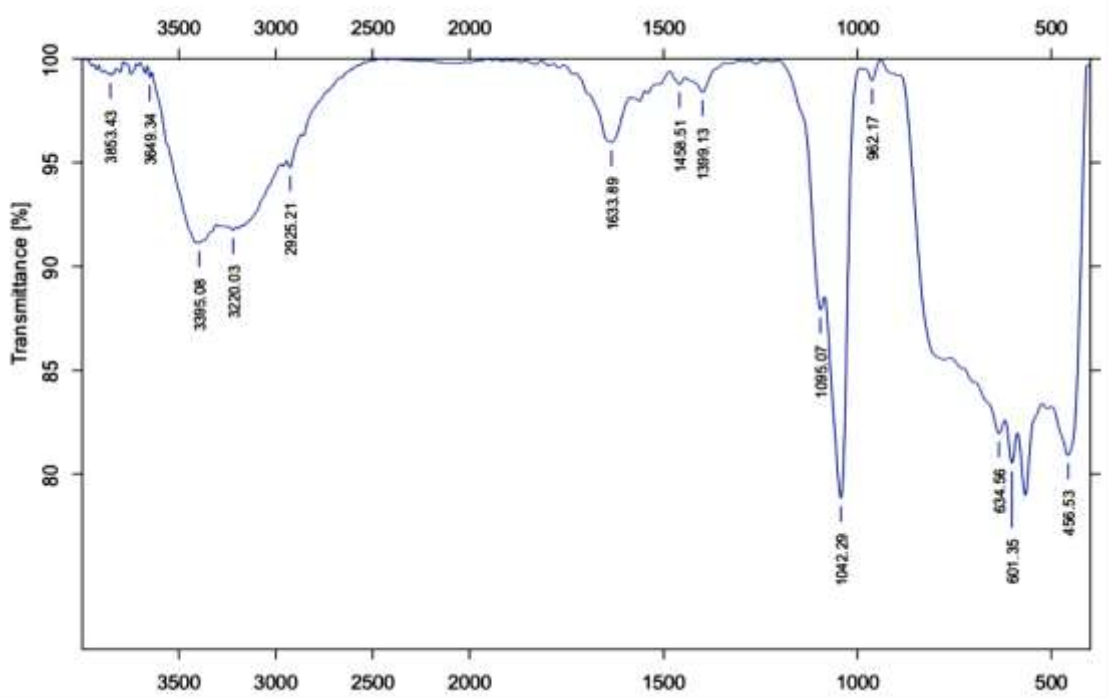

Figure 4. FTIR spectrum of HA/Ag/TiO_2

Survival assay

Viable cells were evaluated by MTT assay, where the viability of cells was determined by the reduction of yellow MTT into purple formazan product by mitochondrial dehydrogenase present in metabolically active cells. Cultured MCF-7 were treated with TNT and HA/Ag/TiO_2 separately (1, 10, 100 µg/ml) for 24 h and 48 h. Table 1 shows IC50 value for MCF-7 cell line treated with TNT and HA/Ag/TiO_2. According to IC50 test, the concentration of HA/Ag/TiO_2 that is required for 50% inhibition of MCF-7 cell proliferation was reduced comparing to concentration of TNT.

Table 1. IC50 value for MCF-7 cells treated with TNT and HA/Ag/TiO_2

Sample	IC_{50}
TNT	110
HA/Ag/TiO_2	98

Figure 5 shows the cell viability after incubation with different concentrations of TNTs for 24 h and 48 h. TNTs did not induce any change in the proliferation with a concentration up to 100 µg/ml, suggesting the absence of toxicity of the TNT. Subsequently the proliferation of MCF-7 cells reduced significantly at a dose of 100 µg/ml, the cell proliferation was reduced by 59% and 57% respectively in 24 h and 48 h exposure times. It is also noted that incubation time on different

concentrations of TNTs did not induce any significant change in the inhibition of cell proliferation.

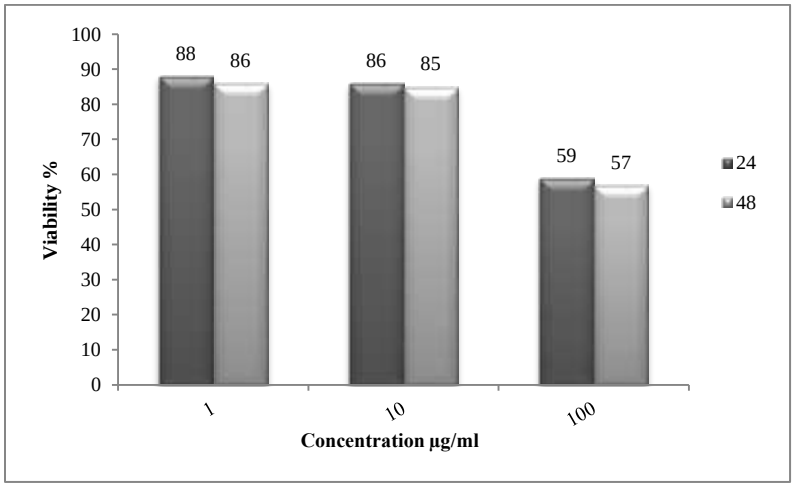

Figure 5. Cytotoxicity of TNT with different concentrations after 24 h and 48 h incubation

Figure 6 shows the cell viability after 24 h and 48 h incubation with different concentrations of HA/Ag/TiO_2. Similar to TNTs, it did not induce any change in the proliferation with a concentration up to 100 µg/ml. Subsequently the proliferation of MCF-7 cells reduced significantly at a dose of 100 µg/ml, the cell proliferation was reduced by 51% and 50% respectively in 24 h and 48 h exposure times. Incubation time on HA/Ag/TiO_2 shows the significant role in the control of cell proliferation.

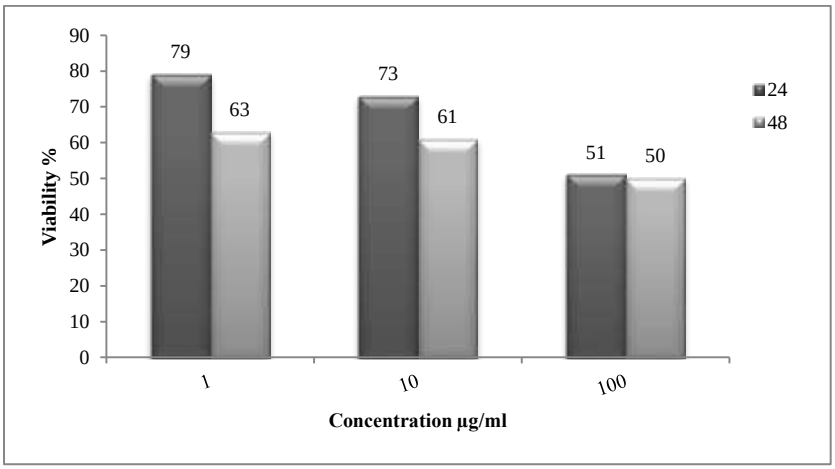

Figure 6. Cytotoxicity of HA/Ag/TiO_2 with different concentrations after 24 h and 48 h incubation

Figure 7 shows the cell viability after 24 h incubation with TNT and HA/Ag/TiO_2. In all the concentration the inhibition of cell proliferation by HA/Ag/TiO_2 is more than pure TNT itself. This strongly indicates that modified TiO_2 act as a more potent anticancer drug than pure TiO_2 .

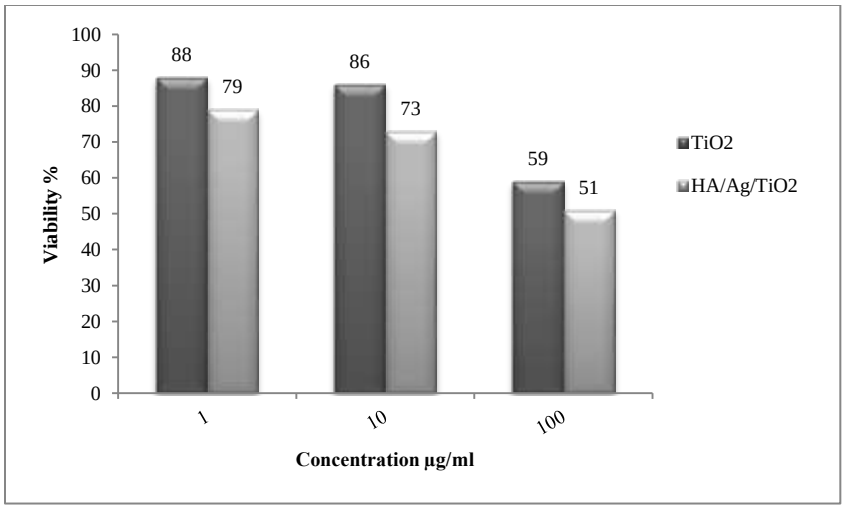

Figure 7. Cytotoxicity of TNT, HA/Ag/TiO_2 with different concentrations after 24 h incubation

Figure 8 shows the cell viability after 48 h incubation with TNT and HA/Ag/TiO_2. In all the concentration with increase incubation duration to 48 h, the inhibition of cell proliferation by HA/Ag/TiO_2 shows significant change than pure TiO_2 (TNT) itself. Incubation time would be the factor to influence on cell proliferation by HA/Ag/TiO_2.

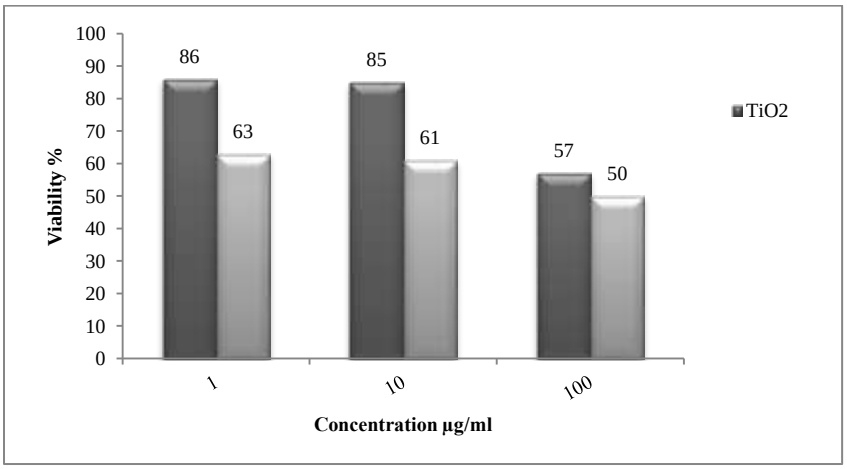

Figure 8. Cytotoxicity of TNT, HA/Ag/TiO_2 with different concentrations after 48 h incubation

CONCLUSIONS

This paper, presents a simple and convenient method to prepare multifunction HA/Ag/TiO_2 order array nanotube as potent to be anticancer drug. The presence of hydroxyapatite and silver particle conjugated to tubular structure of TiO_2 increase the inhibation of MCF-7 breast cancer cell line than TiO_2 nanotube itself and also decrease the IC50 value. The effect of concentration and incubation time of TiO_2 and HA/Ag/TiO_2 on prolirative of MCF-7 cell line was investigated. Thus, the present study will serve as a first step towards investigation the effect of multifunctional composite based TiO_2 as potent anticancer drug on different categories of cells line

ACKNOWLEDGMENTS

We would like to acknowledge the Research Council of Islamic Azad University, Yadegar -e- Imam Khomeini (RAH) Branch for supporting the project entitled "Evaluation of Anticancer activity of nanotube Titanium dioxide modified by nanoparticles (Metal and Metal Oxide)". The authors declare that there is no conflict of interests.

REFERENCES

1. Damodaran V.B., Bhatnagar D., Leszczak V., Popat K.C., 2015. Titania nanostructures: a biomedical perspective. RSC Adv. 5, 37149-37171.

2. Yan J., Zhou F., 2011. TiO_2 nanotubes: Structure optimization for solar cells. J Mater Chem. 21, 9406-9418.

3. Wang X., Li Z., Xu W., Kulkarni S., Batabyal S., Zhang S. Cao A., Lydia Helena Wong L., 2015. TiO_2 nanotube arrays based flexible perovskite solar cells with transparent carbon nanotube electrode. Nano Energy. 11(1), 728–735.

4. Zhang F., Liu Z., Lu W., Lyu C., Lyu C., Wang X., 2015. The Synthesis and Photocatalytic Properties of TiO_2 Nanotube Array by Starch-Modified Anodic Oxidation. Photochem Photobiol. doi: 10.1111/php. 12471.

5. Karthik S., Gopal K., Haripriya E., Sorachon Y., Maggie P., Oomman K., Craig A., 2007. Highly-ordered TiO_2 nanotube arrays up to 220 μm in length: use in water photoelectrolysis and dye-sensitized solar cells. Nanotechnol. 18(065707), 1-11.

6. Jiwon L., Dai Hong K., Seong-Hyeon H., Jae Young J., 2011. A hydrogen gas sensor employing vertically aligned TiO_2 nanotube arrays prepared by template-assisted method. Sensors and Actuators B: Chemical. 160(1), 1494–1498.

7. Sunghoon P., Soohyun K., Suyoung P., Wan In L., Chongmu L., 2014. Effects of Functionalization of TiO_2 Nanotube Array Sensors with Pd Nanoparticles on their Selectivity. Sensors. 14, 15849-15860.

8. Cipriano A.F., Miller C., Liu H., 2014. Anodic growth and biomedical applications of TiO_2 nanotubes. J Biomed Nanotechnol. 10(10), 2977-3003.

9. Kulkarni M., Mazare A., Gongadze E., Perutkova S., Kralj-Iglič V., Milošev I., Schmuki P., Iglič A., Mozetič M., 2015. Titanium nanostructures for biomedical applications. Nanotechnol. 26(062002), 1-18.

10. Park J., Bauer S., Von der Mark K., Schmuki P., 2007. Nanosize and vitality: TiO_2 nanotube diameter directs cell fate. Nano Lett. 7(6), 1686-91.

11. Moisés A.F., Edgar M., Crystel A.S., Ricardo A.G., Pablo Z., Paloma C., Juan M., Diana F., M., Reyes S., T., Cristina R., 2011. Antitumor activity of colloidal silver on MCF-7 human breast cancer cells. J Exp Clin Cancer Res. 29(148), 1-7.

12. Jedd M.H., Arti S., Sherrill A.L., Maximilian B.M., Naomi K.F., Brooke T.M., 2010. Assessing nanotoxicity in cells in vitro. Nanomed Nanobiotechnol. 2(3), 219–231.

13. Grimes C.A., Mor G.K., TiO_2 nanotube Arrays synthesis, properties, and Applications, Springer: New York, 2009.

14. Machida M., Norimoto K., Kimura T., 2005. Antibacterial activity of photo catalytic Titanium Dioxide thin films with photodeposited silver on the surface of sanitary ware. J Am Ceram Soc. 88(1), 95-100.

15. Qiang W., Jin Zh., Lijun Zh., Shimin L., Yanqin L., 2013. Hydroxy apatite coatings for Biomedical Applications, Zhang, S., Ed., Taylor& Francis Group, CRC Press. Pp. 363-430.

16. Mosmann T. 1983. Rapid colorimetric assay for cellular growth and survival: application to proliferation and cytotoxicity assays. J Immunol Methods.65,55–63.

17. Ohno M., Abe T. 1991. Rapid colorimetric assay for the quantification of leukemia inhibitory factor (LIF)

and interleukin-6 (IL-6). J Immunol Methods. 15;145(1-2),199-203.

18. Bailey M.J., Coe S., Grant D.M., Grime G.W., Jeynes C., 2009. Accurate determination of the Ca: P ratio in rough hydroxyapatite samples by SEM-EDS, PiXE and RBS-a comparative study. X-ray Spect. 38, 343-347.

19. Elahifard M.R., Rahimnejad S., Haghighi S., Gholami M.R. 2007, Apatite-Coated Ag/AgBr/TiO_2 Visible-LightPhotocatalyst for Destruction of Bacteria. J Am Chem Soc. 129(31), 9552-9553.

20. Smirnova N.P., Manuilov E.V., Korduba O.M., Gnatyuk Yu.I., Kandyba V.O., Eremenko A.M., Gorbyk P.P., Shpak A.P., 2009. Nanomaterials and Supramolecular Structures: Physics, Chemistry, and application, Anatoliy, P.S., Gorbyk , Eds., Springer, NY. pp. 131-145.

Appendix 1: EDAX Analysis of HA/Ag/TNT

Elt	Line	Int	Error	K	Kr	W%	A%	ZAF	Formula	Ox%	Pk/Bg	Class	LConf	HConf	Cat#
O	Ka	488.3	360.7500	0.1573	0.0848	40.87	65.88	0.2074		0.00	54.67	A	40.32	41.42	0.00
F	Ka	70.2	360.7500	0.0158	0.0085	5.20	7.05	0.1635		0.00	8.62	A	5.01	5.38	0.00
Na	Ka	98.4	41.4401	0.0121	0.0065	1.68	1.88	0.3891		0.00	4.59	A	1.63	1.73	0.00
P	Ka	210.8	17.8639	0.0283	0.0153	1.80	1.50	0.8469		0.00	5.58	A	1.76	1.84	0.00
Cl	Ka	59.9	17.8639	0.0100	0.0054	0.61	0.45	0.8808		0.00	3.11	B	0.59	0.64	0.00
Ca	Ka	182.7	17.8639	0.0416	0.0224	2.26	1.45	0.9942		0.00	6.18	A	2.21	2.31	0.00
Ti	Ka	2151.6	17.8639	0.6203	0.3344	37.80	20.35	0.8844		0.00	61.22	A	37.56	38.05	0.00
Ag	La	55.5	17.8639	0.0217	0.0117	1.44	0.34	0.8126		0.00	3.07	B	1.38	1.50	0.00
Au	La	7.4	0.4251	0.0928	0.0500	8.34	1.09	0.5999		0.00	2.60	B	7.42	9.25	0.00
				1.0000	0.5390	100.00	100.00			0.00					0.00